IMPROVING THE DESIGN OF STEAM TURBINE INLET VALVES BY NUMERICAL METHODS FOR ENHANCED PART LOAD OPERATION

C. B. Domnick[1], F.-K. Benra[1], D. Brillert[1], H. J. Dohmen[1], C. Musch[2]

[1]Chair of Turbomachinery, University of Duisburg-Essen, Duisburg, Germany, bernhard.domnick@uni-due.
[2] Siemens AG, Mülheim an der Ruhr, Germany, christian.musch@siemens.com

ABSTRACT

The flow field of a typical steam valve geometry used for large power stations is computed with CFD methods at different operation conditions. Unsteady CFD calculations using the Zonal-Forced-LES model are performed to model the flow instabilities and the dynamic forces. These time-dependent forces are transferred to highly non-linear time-dependent FEM calculations to analyse the vibration level generated by the dynamic forces.

The flow analysis shows that wall jet separation, shear layer instabilities and acoustic modes contribute significantly to the dynamic steam forces at part load operation. Geometry modifications which affect these phenomena are presented and evaluated at different operation conditions.

NOMENCLATURE

a	Acceleration	[m/s²]	Ma	Mach number	[-]
a_{ref}	Reference acceleration	[m/s²]	p	Pressure	[bar]
c_s	Speed of sound	[m/s]	p_{in}	Inlet pressure	[bar]
D	Diameter	[m]	p_{out}	Outlet pressure	[bar]
F	Force	[N]	$p_{t,in}$	Total inlet pressure	[bar]
F_{ref}	Reference force	[N]	$\hat{p}$	Rel. pressure fluctuation	[-]
f	Frequency	[1/s]	q	Non dimensional mass flow	[-]
h	Gap height	[m]	r	Radius	[m]
j	Mass flux	[kg/(m².s)]	St	Strouhal number	[-]
j*	Critical mass flux	[kg/(m².s)]	Π	Pressure ratio of the valve	[-]
l	Lift of the valve plug	[m]	Π_{Attach}	Pressure ratio of attachment	[-]
$\dot{m}$	Mass flow rate	[kg/s]	Π_{Coanda}	Pressure ratio of Coanda jet	[-]

INTRODUCTION

The power output of steam turbine plants can be controlled by adjusting the pressure in the boiler and throttling the mass flow by steam turbine inlet valves. As the adjustment of the live steam pressure is slow and limited due to the characteristics of the boiler, inlet valves are always necessary to control the power output of a steam turbine. Due to large pressure drops and high mass flow rates, a large amount of energy is dissipated in the valve. Depending on the design of the valve a certain amount of the dissipated energy is converted to sound and vibration.

At part load operation conditions, at which large pressure drops and still high mass flow rates exist, the dissipation is large. At these operation conditions undesired valve vibrations are reported. For instance, Zaryankin [20] investigated valve failures rates of steam turbine inlet valves. The analysis shows, that valves which are used in base load plants have the lowest failure rate. Turbine inlet valves, which are used in cogeneration plants operate more often in part load and have comparatively high mass flow rates due to steam extraction. According to Zaryankin [20] these valves have a failure rate which is 2 to 3 times higher than the failure rate of valves used in base

load plants. The highest failure rate is observed at steam turbines used in chemical plants and steel works which often operate in part load.
As the amount of volatile renewable energy fed into the power grid increases, thermal power stations will have to operate more often in part load. So the operation conditions which are undesired in terms of valve vibration occur more often and research has to be conducted to reduce the valve vibrations at part load operation. Certain parts of steam valves can be damaged at these operation conditions. Kostyuk[8] et al. report destroyed nozzle boxes and valve seats. Zhang et al. [22] report of a valve stem rupture.

Early research on flow induced valve vibrations using scaled models was done by Heymann [6] in the seventies. Measurements in model valves show, that the sound generated by the valve depends on the flow topology and on the operation point. Two flow topologies are distinguished by Haymann. These are the attached flow topology and the detached flow topology. The detached flow generates a significantly higher sound level than the attached flow. The reason for the transition between the two topologies could not be clarified at that time. Later investigations by the Domnick et al. [3] of a similar valve geometry show, that the transition of the flow topology is related to the Coanda effect. It is also shown, that the flow topology correlates with the vibrational level of the steam valve. In case of the detached flow, the vibrations measured at the steam valve are significantly higher than in case of attached flow.
Besides wall jet separation other fluid dynamic phenomena can cause undesired dynamic steam forces and vibration. Several researchers as Nakano [13], Ziada [23] and Widell [18] report of acoustic modes which are excited in valves and generate undesired vibration or noise. Depending on the geometry of the valve, different mechanisms exist, which can excite the mode. These can be for instance oblique or normal oscillating shocks, jet instabilities or fluid structure interaction.

Other researchers report that normal shocks, which exist at certain operation conditions in convergent-divergent valve gaps, can cause severe valve vibration if they start to oscillate. The investigations of Pluviose [15], Stastny [16] and Zhang [21] show that dynamic forces and pressure pulsations are significantly reduced if the shape of the valve gap is changed from convergent-divergent to pure convergent. In this case the shock cannot exist in the valve gap where it can impress high dynamic forces directly to the valve plug.

If hemispherical shaped valve plugs are used, strong dynamic forces can arise due to asymmetric flow separations from the valve plug. Comprehensive experimental as well as numerical research on this topic is done by Morita et al. [12] who observed the transient behavior of the flow and determined the operational range at which the asymmetric flow separation occurs. Additionally Zanazzi [19] contributes to a better understanding of the flow field by conducting unsteady simulations in which the SAS turbulence model by Menter [11] is applied. Zhang and Engeda [21] compare a mushroom type valve plug to flat bottom valve plug and show that the flat bottom Valve plug is favorable in terms of dynamic load and vibration.

A further effect that can cause valve vibration is vortex shedding. Usually vortex shedding mechanism is coupled to another effect that triggers the separation of vortices. For instance Darwish and Bates [2] report of vibration in a steam check valve in which the vortex shedding is coupled to a torsional mode of the valve actor. Janzen [7] et al. report of noise and vibration problems caused by vortex shedding in a gate valve. In this case the vortex shedding is coupled with acoustic modes.

These examples show, that various mechanisms exist, that can cause valve vibration. In several cases two or more effects generating vibration coexist and amplify each other. Due to that comprehensive unsteady numerical simulations are necessary to capture the effects generating vibrations.

BASELINE DESIGN OF THE VALVE

The baseline design is a characteristic design of a steam valve as installed in large power stations. If this valve is operated in the admissible range of design mass flow, vibration can be clearly measured but the vibrational level does not exceed the acceptable level.

In the CFD analysis the control valve section shown in fig. 1 is analyzed. The steam enters the control valve section at the inlet (A) coming form an annular chamber which is not part of the CFD domain. The influence of this chamber on the flow field at the valve plug is negligible according to a previous study of the authors [3]. The flow passes by four flow straighteners (B) which are installed directly upstream the valve. It then passes by the valve plug (C) and flows through the diffuser outlet (F) which is connected to the steam turbine. The back cavity of the valve (D) is connected by four bores (E) to the main flow path to enable a fast movement of the valve plug.
In the structural analysis the dynamics of the valve plug and the actuator are investigated. Piston rings (I) are inserted in the valve plug (C) to avoid leakage flows and to damp vibration. The plug is operated by a hydraulic actuator. A spring package (H) ensures that the valve is closed if the hydraulic cylinder (G) is depressurized. At 100% lift the plug is completely retracted and the valve is opened. At 0% Lift the valve is closed.

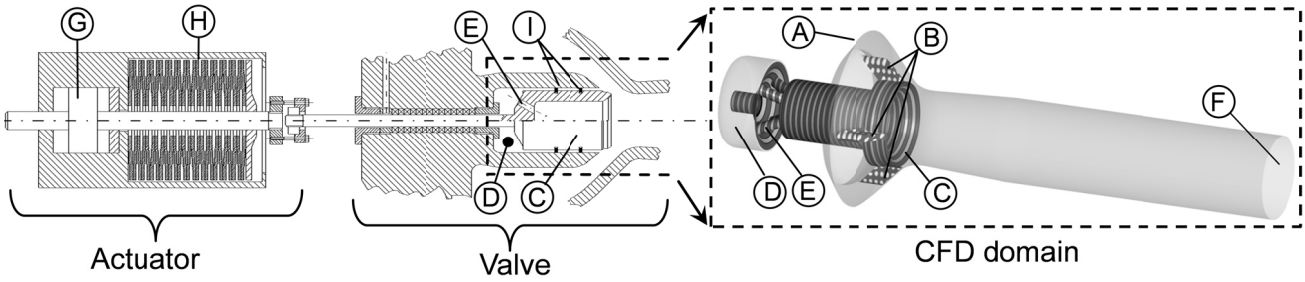

Fig.1: Sketch of the valve and the actuator (not to scale) and the CFD domain

NUMERICAL SETUP

The numerical investigations are performed using the commercial code Ansys® CFX 14. This code applies a fully coupled implicit Navier-Stokes solver. The finally chosen transient numerical set up is second order accurate in time and space. The computational domain is discretized by block structured hexahedral grids. The non-dimensional wall distance (y^+) of the first node is below 30 in the valve diffuser and the boundary layer is resolved by at least 20 nodes. Due to that and due to the high spatial resolution in regions with supersonic flow the computational grids are large. The number of nodes in the base line geometry reaches up to 18 million nodes. Additionally a very small time step of 0.01ms has to be used according to previous work of the authors [4]. So the transient simulations, which are conducted to obtain the dynamic forces acting on the valve plug are time intensive. It takes 2 month of computational time on 20 cores to simulate 80 ms of the steam flow at one operational point. After 30ms simulated time a constant transient level of pressure fluctuations is reached. The transient data for the averaged and fluctuation quantities is extracted after this point.

As steam has a strong real gas behavior at typical operation conditions for coal fired power stations, the fluid properties of the superheated steam are modeled according to the IAPWS model by Wagner et al. [17]. The turbulence model has a huge influence on the dynamic forces which are computed. A comprehensive study on the selection of the turbulence model has been performed by Domnick et al. [4]. This study shows that the SAS-F turbulence model has the best agreement to validation cases that comprise flow instabilities which also occur in the steam turbine inlet valve. Additionally Musch [14] showed in a comparison of simulation data to test rig measurements that the major dynamic flow effects in a steam turbine valve are reproduced by this model. In contrast to a full large eddy simulation the SAS-F model relies in the boundary layer on the RANS formulation. As the separation of the jet flow investigated in this study is caused by a shock related to the expansion and recompression structure of the supersonic jet and not by frictional losses, the simple URANS approach in the boundary layer is assumed to be sufficient for this case. As large-eddy-simulations are significantly more time consuming and the SAS-F model is able to reproduce the characteristic pressure fluctuations, this model is used in this study.

The structural dynamics are computed by ANSYS14. The FEM model includes the valve plug, the coupling and the valve actuator. As the bearings, which guide the valve stem and the valve plug, have a certain clearance, the plug and the stem can also be displaced in radial direction. This effect is modeled in the FEM calculations by defining contact surfaces. Additionally piston rings and a packing (I) exist in the valve, which impress frictional forces on the valve plug. These frictional forces are also modeled by contact surfaces. The spring package (H) is modeled by an analogous body. Due to the frictional effects and the contacts, the FEM model is nonlinear. Hence it is solved in the time domain. An implicit solver using the Newmark interpolation scheme is applied. A detailed description of the implicit numerical scheme is described by Chung and Hulbert [1]. The dependency of the elastic modulus on the temperature is accounted by defining temperature dependent material properties and a temperature distribution in the valve plug.

WALL JET SEPARATION

From operational experience it is known, that the valve discussed here, shows some vibration at low part load operation. This vibration is acceptable if the operation curve of the valve is within the admissible range. An example for this kind of vibration is given in fig. 2 which shows operational records of two power stations. It shows the normalized vibration, the pressure ratio and the lift of the valve plug while the power output of the plant is increased. At the beginning of the operational record, the pressure ratio and the lift are low and the vibration is high. During a constant increase of lift and pressure ratio the vibrational level is reduced suddenly. These transition points (TPs) can be reproduced in a single plant but they differ between power plants with different design flow rate.

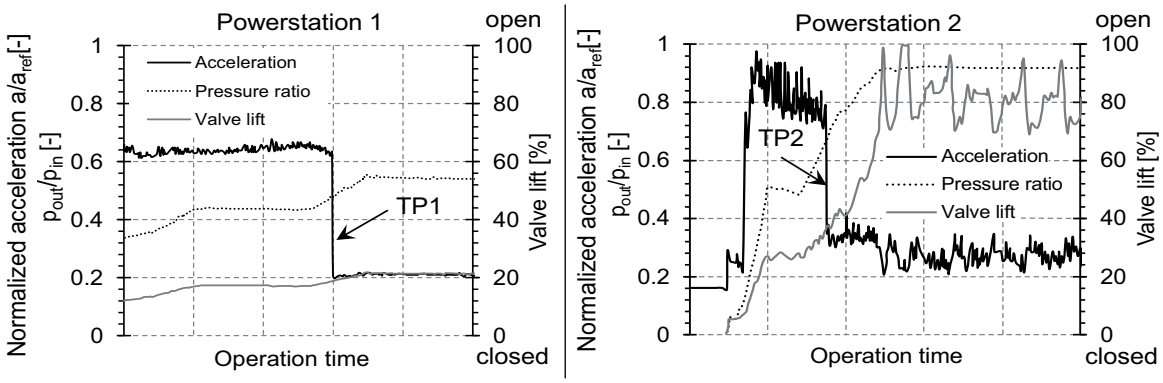

Fig. 2: Operational records showing transition points at partload operation

Steady state CFD analysis

Steady state CFD calculations, which are performed prior to the unsteady calculations show that two major flow topologies exist at part load operation in the steam valve diffuser. As in the case described by Heymann[6] the flow can be attached or detached. In case of the attached flow, the jet formed in the valve gap between the valve seat and the valve plug attaches to the seat and the subsequent diffuser. In case of detached flow the jet is separated from the seat by an oblique shock and flows into the center of the diffuser. The oblique shock results from the under expansion of the supersonic jet having expansion and recompression zones. At low overall pressure ratios the local pressure in the region of the valve seat is smaller than the pressure in the valve gap forming the jet. Hence the jet expands directly after the valve gap. Due to the nature of the supersonic jet, the pressure in the first expansion zone drops below the pressure of the surrounding steam. This causes a subsequent recompression which forms a shock causing the separation if a certain degree of under expansion is exceeded.

The pressure ratio, at which the detached jet attaches, is determined in CFD calculations by increasing the pressure ratio gradually at a constant lift of the plug. This procedure is repeated at different lifts. The results are plotted in fig. 3, which shows that the pressure ratio of attachment increases with increasing lift of the valve plug. The pressure ratio of the valve is defined in eq. (1).

$$\pi = \frac{p_{out}}{p_{t,in}} \tag{1}$$

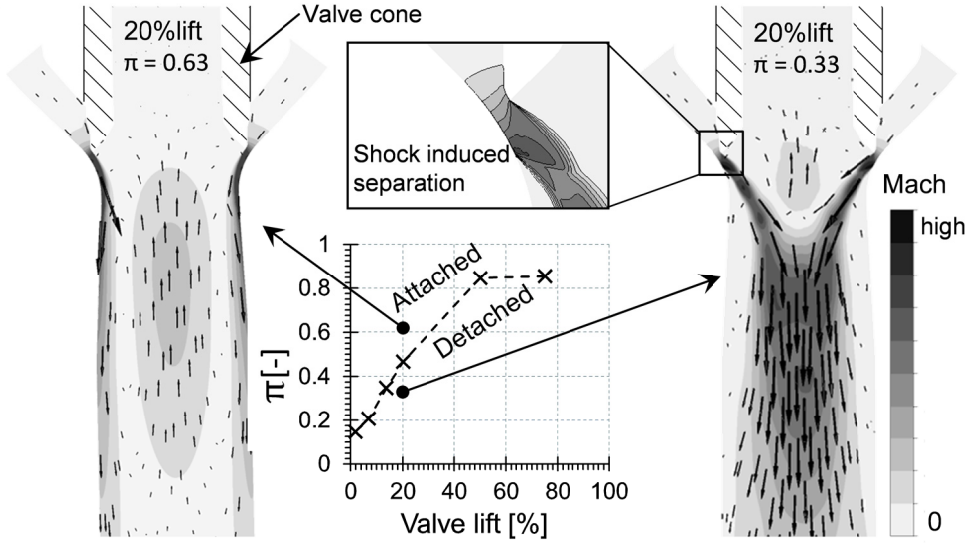

Fig. 3: Transition from the attached to the detached flow topology

This behavior is related to the Coanda effect causing the attachment of the jet. A detailed investigation on that can be found in Domnick et al. [3]. Basic research experiments regarding the Coanda effect show that the pressure ratio at which a detached jet attaches to a circular surface depends on the radius to jet height ratio (r/h-ratio). The basic setup of these investigations and the definition of the geometric ratio are shown in fig. 4. The measurements obtained by different researchers are depicted in fig. 4 agree well. Also the points of attachment determined in the CFD calculations are plotted into this diagram. As the pressure close to the jet determines the separation, the local pressure ratio is extracted from the CFD calculations. It is obtained by dividing the pressure beneath the valve plug by the total pressure at the inlet of the valve. It differs from the overall pressure ratio as the pressure in the diffuser increases from the valve seat region to the outlet. The r/h-ratio is obtained from the curvature of the valve seat and the height of the gap formed by the seat and the plug. The attachment observed in the CFD is close to the Coanda wall jet attachment curve. Thus it can be concluded that the flow transition is caused by the Coanda effect.

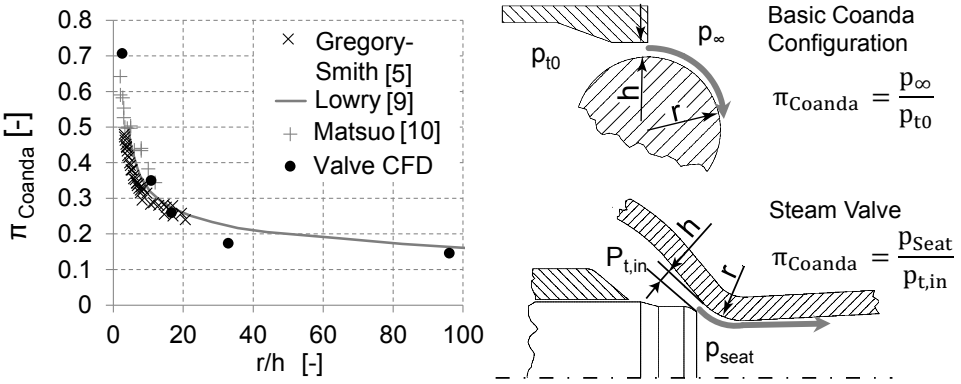

Fig. 4: Comparison of the flow attachment in the valve diffuser to the Coándá wall jet attachment

Based on the pressure ratio of attachment, which is known from the basic research and based on pressure recovery correlations of the valve diffuser the curve of attachment can be computed. It is drawn into the characteristic chart of the valve. The non-dimensional mass flow rate in fig. 5 is defined in Equation (2). j^* is the critical mass flux obtained from the inlet conditions.

$$q = \frac{\dot{m}}{D^2_{\text{Valve seat}} \cdot \frac{\pi}{4} \cdot j^*} \tag{2}$$

Additionally, the operating curves of the two valves whose vibration is shown in fig. 2 are plotted in fig. 5. The transitional points at which the vibration suddenly drops are demarked on these curves. As these points are close to the intersection with the line of attachment, the high vibrational level can be related to the detached jet and the low level can be related to the attached jet.

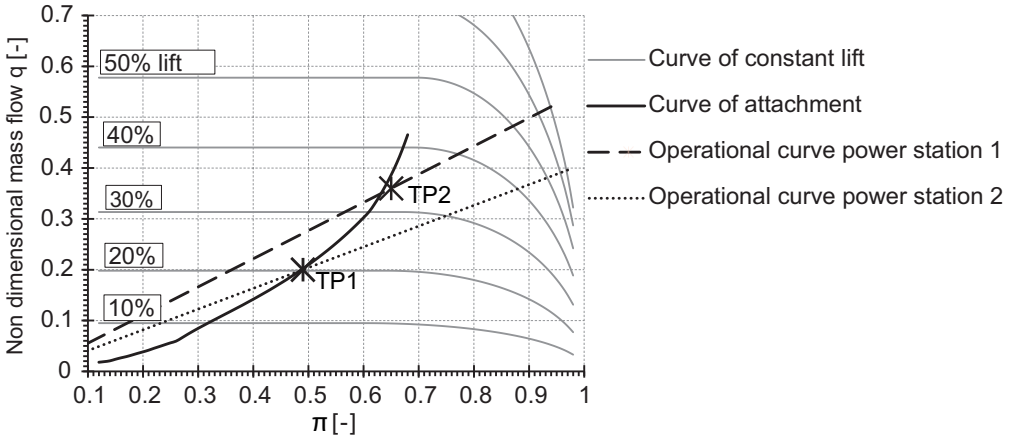

Fig. 5: Comparison between topology prediction tool and measured transition points

Unsteady analysis

To clarify the effects generated by the pressure fluctuations, unsteady CFD simulations are performed. The flow is investigated at 20% lift. The attached as well as the detached flow topology are analyzed. The dynamic forces generated by the flow are transferred to the FEM to investigate the vibrational behavior.

The unsteady investigation reveals that the attached and the detached flow topology can be subdivided into sub-topologies. The sub-topologies, which depend on the pressure ratio, are shown in fig. 6. At pressure ratios which are significantly higher than the pressure ratio of attachment the completely attached wall jet can be found. In this case the dynamic transverse forces which are shown in fig. 7 are low. If the pressure ratio is close to the pressure ratio of attachment, the entire jet is attached, but a separation bubble appears. In this case the transverse forces are significantly higher than in the case of the completely attached wall jet. If the pressure ratio is beneath the pressure ratio of attachment, the jet detaches from the wall. Just beneath the pressure ratio of attachment the separated jet reattaches asymmetrically to the wall of the valve diffuser. In this case the highest dynamic transverse forces can be found. The asymmetric pattern is caused by an asymmetric pressure distribution at the valve seat. The jet tends to reattach in regions where the local pressure is slightly higher and causes thereby strong pressure fluctuations. In reverse the asymmetric flow pattern maintains the asymmetric pressure distribution. A more detailed discussion on the asymmetry can be found in Domnick et al. [4]. At pressure ratios significantly lower than the pressure ratio of attachment the jet remains detached and flows in the center of the diffuser. With increasing distance to the pressure ratio of attachment, the intensity of the dynamic transverse force decreases. The dynamic axial force shown in fig. 8 primary depends on the overall pressure ratio. With decreasing pressure ratio the dynamic axial force increases.

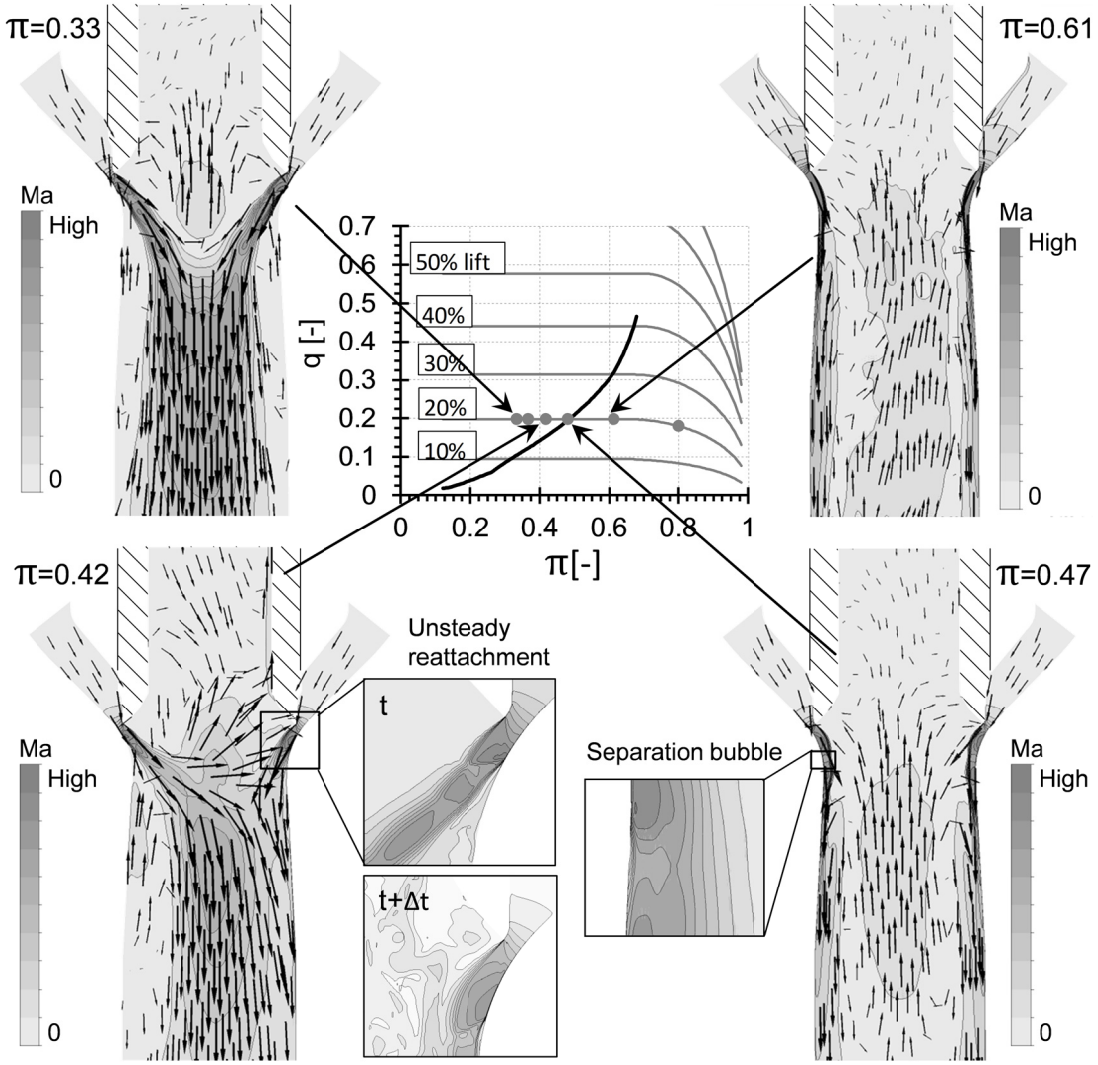

Fig. 6: Time averaged flow field in the steam valve diffuser

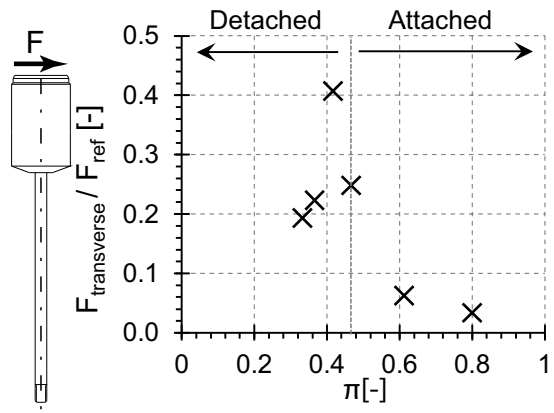

Fig. 7: Root mean square (RMS) value of the transverse force

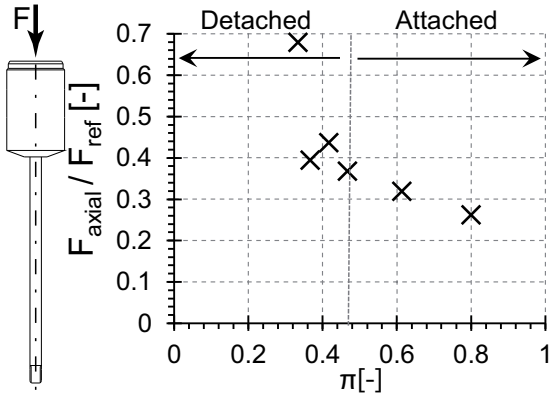

Fig. 8: RMS value of the axial force

The dynamic loads obtained by the CFD simulations are impressed on the mechanical model to obtain the response to the excitation by the dynamic forces. Besides the dynamic forces of the flow field also the friction forces at the piston rings vary. The pressure distribution at the piston ring and hence the normal force is known from an experimental investigation. Based on scaling laws, the forces at the valve are calculated. According to Coulomb's law of friction the friction forces are

obtained. The frictional forces increase with increasing pressure ratio over the piston rings. The dependency of the frictional forces on the pressure ratio is depicted in fig. 9.

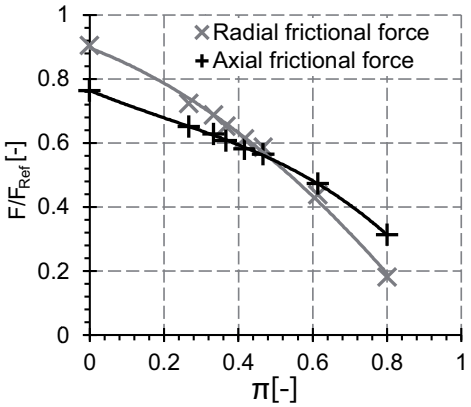

Fig. 9: Frictional forces of the piston rings

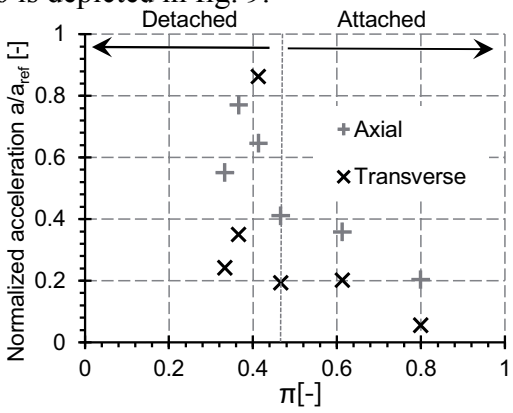

Fig. 10: RMS value of the vibrational acceleration at the coupling

The vibrational acceleration at the coupling of the valve obtained by the FEM is depicted in fig. 10. A clear transition in the transverse vibrational acceleration exists at the pressure ratio of attachment. This behavior correlates with the transition of vibration observed in the power stations. The axial vibration increases with decreasing pressure ratio down to a pressure ratio of 0.36. From the pressure ratio of 0.36 to the pressure ratio of 0.33 the axial vibration decreases. This can be explained by the frictional forces which increase with decreasing pressure ratio.

The investigation shows, that the highest transverse force and vibrations are generated when the asymmetric reattachment of the detached wall jet occurs. This happens just before the complete attachment occurs. Measurements from power plants show that sudden transition in the vibrational level can be related to this effect.

IMPROVING THE JET ATTACHMENT

The wall jet separations related to the Coanda effect can be reduced by reducing the curvature of the valve seat. If the radius of curvature of the valve seat is increased, the r/h-ratio determining the pressure ratio of attachment increases as well. The contours of the standard and the improved design are shown in fig.11. The pressure ratio of attachment of both geometries is drawn versus the lift of the valve plug in fig. 11. The diagram shows that the less curved valve seat yields in a reduction of the pressure ratio of attachment at the investigated range of the lift. Thus, the curve of attachment is shifted to a lower level and the operational curve intersects it at a lower pressure ratio. So the separation occurs at low pressure ratios at which the frictional forces of the piston ring are higher and less power is dissipated in the valve.

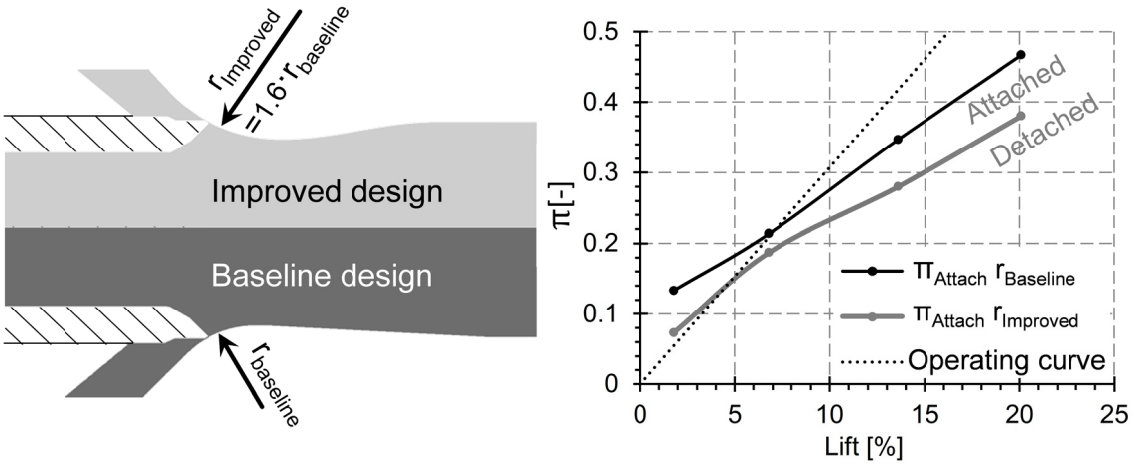

Fig. 11: Design of the improved valve seat and impact on the pressure ratio of attachment

ACOUSTIC DESIGN OF THE BACK CAVITY

In the axial force spectra of the three operating points with the attached flow topology distinct peaks exist. The force spectra are shown in fig. 12. In this figure the frequency is expressed by the Strouhal number defined in eq. (3). c_s is the speed of sound. Although the pressure ratio differs in these cases, the frequency of the peak remains nearly constant. This indicates that this peak is related to an acoustic mode.

$$St = \frac{f \cdot D_{Seat}}{c_s} \tag{3}$$

In addition pressure fluctuations exist in the back cavity of the valve. These fluctuations are plotted in fig. 14. As the velocity is very low in this part of the valve, the pressure cannot be generated directly by flow instabilities in the back cavity. So the pressure fluctuations have to be transferred from a distant part of the valve to the back cavity by acoustic effects.

To clarify that mechanism, an additional modal computation, predicting the eigenshapes of the gas volume in the valve, is performed. The solver ANSYS Mechanical, which is also capable of solving the wave equation in a gas volume, is used for this computation. An eigenmode, which resembles the pattern of pressure fluctuations well, exists at St=0.07. This Strouhal number is close to the Strouhal number of the frequency peak. So this mode is found to be the source of the pressure peak.

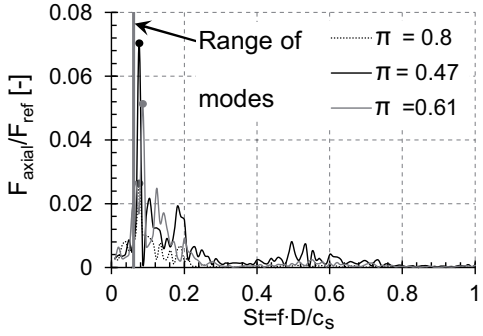

Fig. 12: Axial force spectra of the attached flow

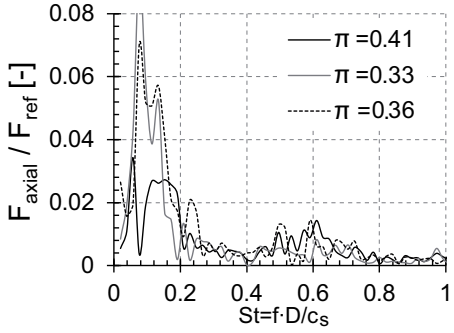

Fig13: Axial force spectra of the detached flow

In contrast to that, the spectra of the dynamic axial loads generated by the detached flow topology are much broader. A single peak which is significantly higher than the other peaks and that contributes significant to the dynamic forces cannot be found in the spectra plotted in fig. 13.

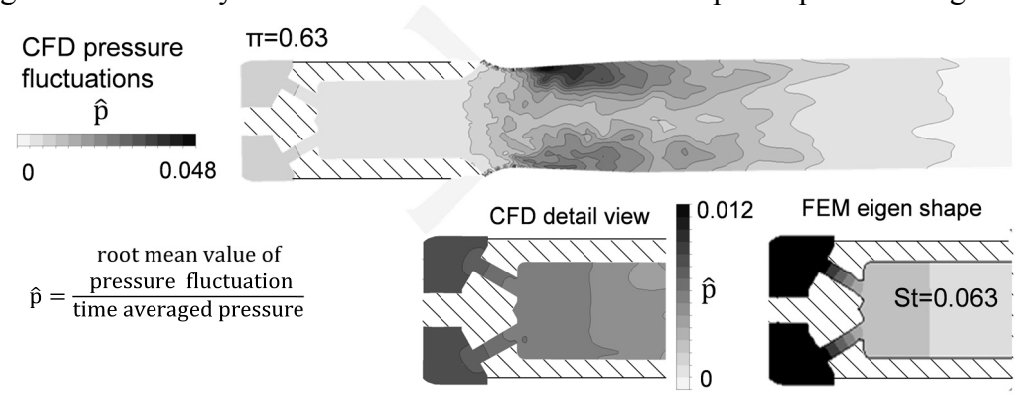

Fig. 14: Comparison between pressure fluctuations and the modal eigenshape in the back cavity

The finding that the acoustic mode in the back cavity contributes significantly to the dynamic forces in certain cases is used to optimize the shape of the plug. Two generic geometries are analyzed to show the potential for improvement. In the first geometry, the diameter of the bores con-

necting the back cavity to the main flow path is increased. This increases the cross-sectional area connecting the back cavity to the main flow path by 146%. The second design variant compromises three ribs connecting the stem to the valve plug. In this case the cross sectional area is increased by 800% compared to the baseline design.

The three designs are shown in fig. 15. CFD simulations are carried out for a pressure ratio of 0.633 and a pressure ratio of 0.333. In case of the attached flow at a pressure ratio of 0.633, the intensity of the dynamic forces is reduced. Especially the low frequency content with a high potential of excitation is reduced by the improved geometries.

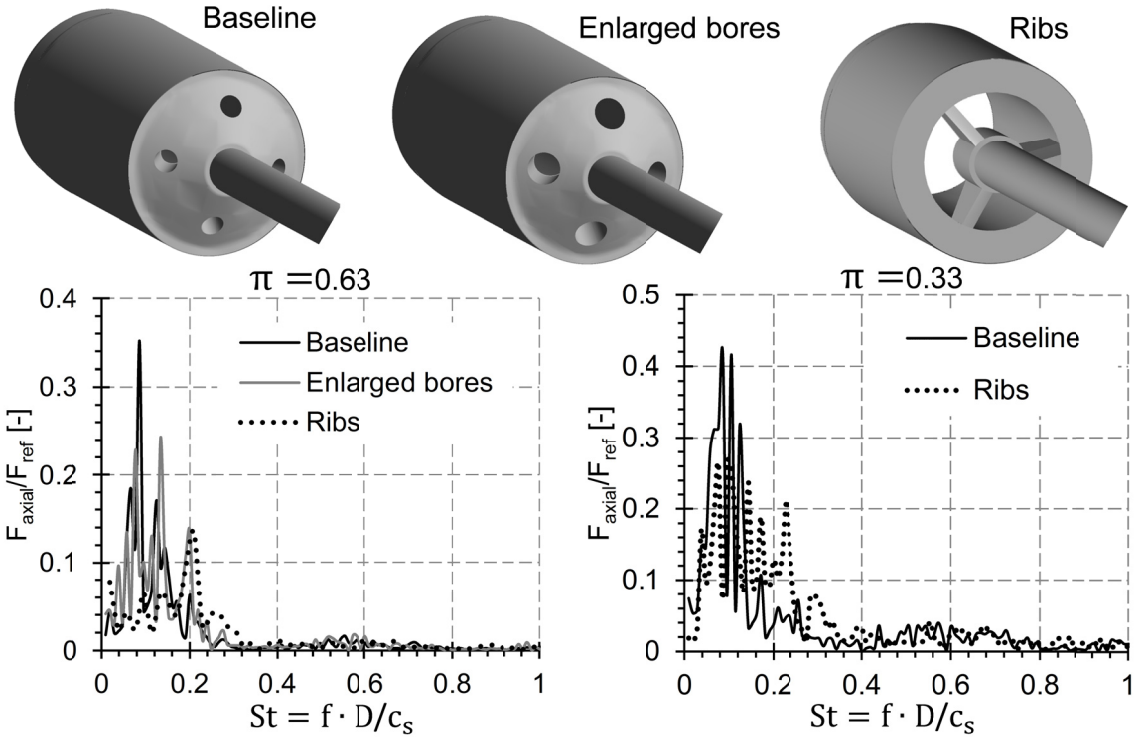

Fig. 15: Design variants of the valve plug and corresponding force spectra

As the design with the ribs achieves the highest reduction of dynamic forces in case of the attached flow, it is also tested for detached flow. Compared to the attached flow case, the reduction is smaller in the case of the detached flow. The strongest peaks are moderately reduced but the spectrum is broader. The major reason for this is, that the design with the ribs aims on reducing the effect of the acoustic mode in the back cavity of the valve and this mode is not the predominant source of dynamic axial force in case of detached flow.

The dynamic forces obtained from the CFD calculations are impressed on the FEM. The resulting vibration obtained by the FEM calculation is shown in fig. 17. In case of the attached flow, both the axial and the transverse vibration are reduced. In case of the detached flow, the design of the valve plug has only little effect on the vibrational level.

REDUCING THE EXCITATION OF THE SHEAR LAYER

If the flow is attached, a shear layer exists between the high speed wall jet and the back flow in the center of the diffuser. The strong backflow is caused by the entrainment of the jet. The CFD simulation of the baseline design, which compromises the flow straighteners, shows that this shear layer is disturbed by vortices generated by the flow straighteners. The disturbed shear layer at cross section A of the diffuser is depicted in the center of fig. 16. The straighteners are originally designed to avoid the formation of swirl. In the first step the flow straighteners are removed from the design to examine their effect on the flow and the shear layer. This design variant is shown in fig. 16. In this case, the vortices do not exist and the flow field is much more homogeneous compared to

the baseline design. The formation of swirl is not observed, but the dynamic force of the attached flow ($\pi = 0.63$) is increased.

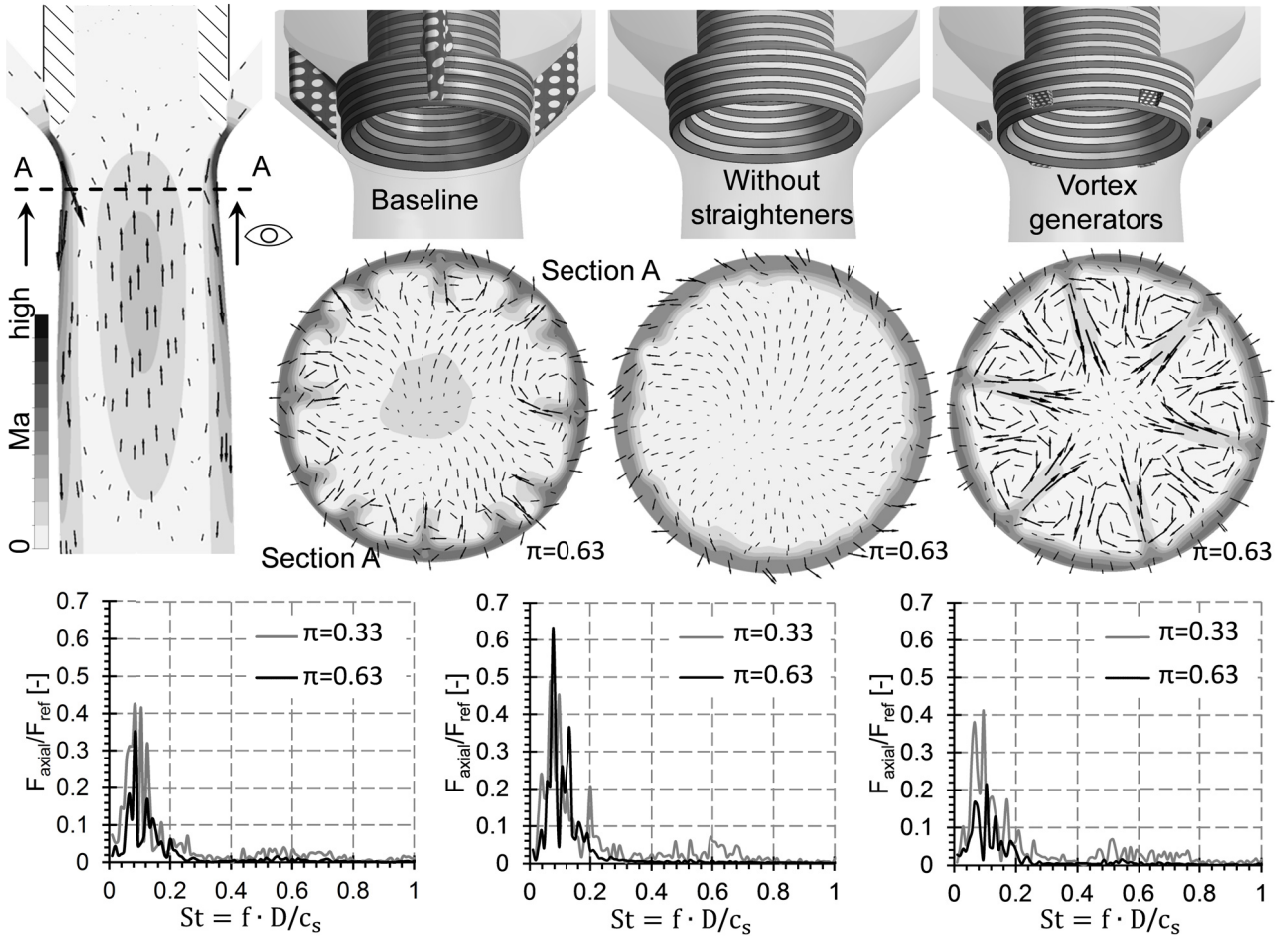

Fig. 16: Geometry of the design variants, time averaged velocity in the Section **A** and axial force spectras of the different design variants

The force spectra are depicted in the lower part of fig. 16. Especially the peak related to the acoustic mode is increased compared to the baseline design. In contrast to that, the axial force spectrum of the detached flow ($\pi = 0.33$) changes moderate and no substantial differences are observed. This two cases show that the shear layer in the diffuser excites the acoustic mode in the back cavity of the valve. If the shear layer is disturbed, the intensity of the acoustic mode is reduced. In case of the detached flow topology, which does not comprise the shear layers, the straightener has no major impact on the dynamic forces and the acoustic mode is not the predominant source of the dynamic force.

As the flow straightener is originally not designed to disturb the shear layer a design variant with improved vortex generating devices is designed. These so called vortex generators depicted in fig. 16, are installed just upstream the valve gap. The vector plot in section A indicates that the shear layer is more disturbed by this design than by the baseline design. Also the main peak of the force spectrum in case of attached flow ($\pi = 0.63$) is reduced significantly. The impact of the design on the force spectrum is smaller when the flow is detached ($\pi = 0.33$), no major differences are observed between the designs in this case.

Again the effect on the dynamic forces on the structure is studied to evaluate the aerodynamic improvement. In fig. 18 the vibrational acceleration at the coupling of the valve stem is shown for the baseline design and for the design with vortex generators. The level is decreased if the vortex generators are used, but the change of design has only little impact on the axial vibration in case of the detached flow. In case of the attached flow a clear reduction of the dynamic axial forces is

found. In addition the transverse forces are reduced in the two analyzed operating points by the improved design.

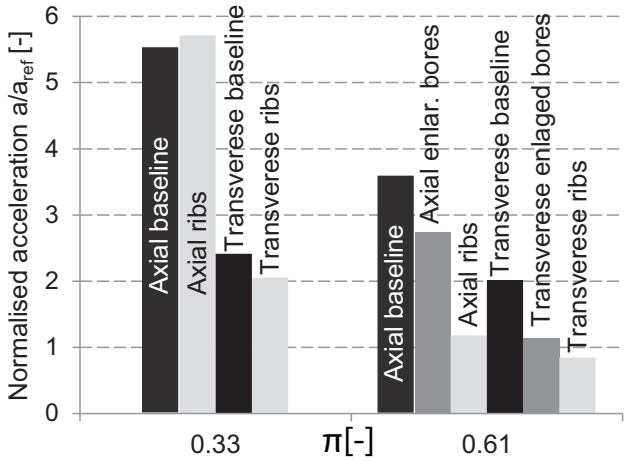

Fig. 17: RMS value of the vibrational acceleration at the coupling of the design variants generated by the attached and the detached flow

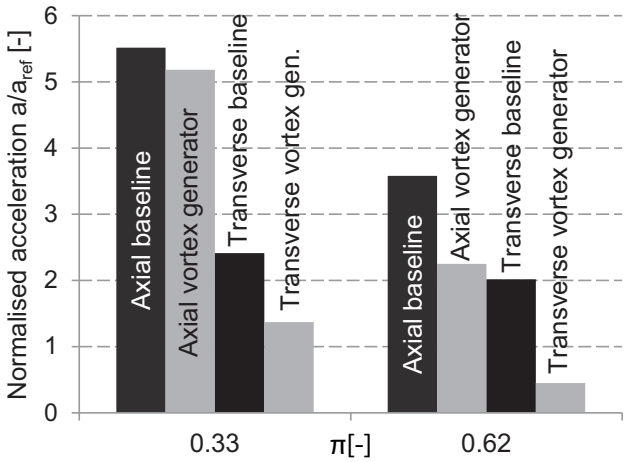

Fig. 18: RMS value of the vibrational acceleration at the coupling of the baseline design and the improved design at two operating points

CONCLUSIONS

The major flow phenomena, generating pressure fluctuation and hence vibration at part load operation, are analyzed using CFD and FEM methods. The attachment of the wall jet in the steam diffuser predicted by CFD correlates with sudden drops in valve vibration observed in power stations. The attached wall jet is favorable as it causes less vibration. As the desired attachment of the wall jet is related to the Coanda effect, the relative wall curvature at the valve seat determines the attachment of the jet to the valve seat. Thus the attachment of the jet can be improved if the seat is less curved.

If the flow is attached, an acoustic mode contributes significantly to the axial forces and to the axial vibration of the valve stem. This mode excited by the shear layer in the valve diffuser impresses in the back cavity of the valve dynamic pressure forces on the valve plug. For attached flow the dynamic axial forces and the vibration can be reduced by acoustically improved plugs with large cross section connections to the back cavity. Also the excitation of the mode can be reduced by disturbing the shear layer that excites the mode in case of attached flow. But both methods of design improvement show significant less impact on the axial vibration if the flow is detached. So the crucial point in improving this valve geometry is the avoidance of the wall jet separation, which leads to undesired transverse vibration. If the attached flow is ensured in a wide operational range, shear layer disturbance and using acoustically improved plugs can provide less axial vibration.

ACKNOWLEDGEMENTS

This work is conducted as a part of the joint research program COOREFLEX-Turbo in the frame of AG Turbo. The work is supported by the German ministry of economy and technology under grant number 03ET7020A. The authors gratefully acknowledge Siemens AG for their support and permission to publish this paper. The responsibility for the content lies solely with the authors.

REFERENCES

[1] J. Chung, G. M. Hulbert (1993), A Time Integration Algorithm for Structural Dynamics with Improved Numerical Dissipation - the Generalized-Alpha Method, *Journal of Applied Mechanics*, 60, *371-375*

[2] M. Darwish, C. L. Bates (1977), Flow Vortex Shedding Forces in Check Valves, *Advances in Instrumentation Part 4, ISA Conf. and Exhibit,* 32, 79-91
[3] C. B. Domnick, et al. (2014), Numerical investigation on Under Expanded Wall Jet Separation in a Steam Turbine Valve Diffusor, *ISROMAC 15*, February 24-28, 2014 Honolulu Hawaii, Paper No. TU305
[4] C. B. Domnick, et al. (2014), Numerical Investigation on the Time Variant Flow Field and Dynamic Forces Acting in Steam Turbine Inlet valves, *Proceedings of ASME Turbo Expo 2014,* GT2014-25632
[5] D. G. Gregory-Smith, A. R. Gilchrist (1987), The compressible Coanda Wall Jet – an Experimental Study of Jet Structure and Breakaway, *International Journal of Heat and Fluid Flow*, 8, 156-164
[6] F. J. Heymann, and M. A. Statiano, (1973), Steam Turbine Control Valve Noise, *85th Meeting of the Acoustical Society of America*.
[7] V. P. Janzen et al. (2007), Acoustic Noise Reduction in Large-Diameter Steam-Line Gate Valves, *2007, ASME Pressure Vessels and Piping Division Conference,* San Antonio Texas
[8] A. G. Kostyuk et al. (2000), An Experimental Analysis of Pressure Pulsations in the Steam Admission Elements of a Turbine Installation, *Thermal Engineering,* 47, 529-537
[9] J. G. Lowry, J. M. Riebe, J. P. Campbell (1957), The jet augmented flap, *Annual meeting of the Institute of Aeronautical Sciences*, New York
[10] S. Matsuo et al. (1998), Study on the Characteristics of Supersonic Coanda Jet, *Journal of Thermal Science,* 7(3), 165-175
[11] F. Menter, Y. Egorov (2005), A Scale–Adaptive Simulation Model using Two-Equation Models, *43rd AIAA Aerospace Sciences Meeting and Exhibit,* Reno Nevada
[12] R. Morita, et al. (2007) CFD Simulations and Experiments of Flow Fluctuations Around a Steam Control Valve, *Journal of Fluids Engineering*, 129, 49-54
[13] M. Nakano et al. (1988), Noise and Vibration related to the Patterns of Supersonic Annular Flow in a Pressure Reducing Gas Valve, *Journal of Fluids Engineering*, 110, 55- 61
[14] C. Musch et al. (2014), A New Emergency Stop and Control Valve Design - Part 2: Validation of Numerical Model and Transient Flow Physics, *Proceedings of ASME Turbo Expo 2014,* GT2014-25117
[15] M. Pluviose (1989), Stabilization of Flow Through Steam-Turbine Control Valves, *Transactions of the ASME*, 111, 642-646
[16] M. Stastny et al. (2003), Pulsating Flows in the Inlet of a Nuclear Steam Turbine, *5th European Conference on Turbomachinery, 677-686*
[17] W. Wagner et al., The IAPWS Industrial Formulation 1997 for the Thermodynamic Properties of Water and Steam, *ASME J. Eng. Gas Turbines and Power*, 122, 150-182
[18] K. E. Widell (1980), Governing Valve Vibrations, In: *Practical Experiences with Flow Induced Vibrations*, (E. Naudascher, D. Rockwell), Springer-Verlag Berlin, 320-322,
[19] G. Zanazzi et al. (2013), Unsteady CFD Simulation of Control Valve in Throttling Conditions and Comparison to Experiments, *Proceedings of the ASME Turbo Expo 2013*, GT2013-94788
[20] A. E. Zaryankin, B.P. Simonov (1996), New Control Valves for Steam Turbines, Their Characteristics and Experience with their Operation, *Thermal engineering*, 43, 19-24.
[21] D. Zhang, A. Engeda (2003), Venturi valves for steam turbines and improved design considerations, *Proceedings of the ASME Part A, Power and Energy*, 217, 219-230
[22] D. Zhang, et al. (2004) Experimental Study of Steam Turbine Control Valves, *Proceedings of the Institution of Mechanical Engineering Science*, 218, 493-507
[23] S. Ziada, E. T. Bühlmann (1989), Flow Impingement as an Excitation Source in Control Valves, *Journal of Fluids and Structures*, 3, 529-549